Article ID: 1006-8775(2020) 03-0321-15

Squall Line and Its Vertical Motion Under Different Moisture Profiles in Eastern China

ZHENG Lin-lin (郑淋淋) [1, 2, 3], SUN Jian-hua (孙建华) [4, 5], ZHANG Jiao (张 娇) [1], QIU Xue-xing (邱学兴) [1], YAO Chen (姚 晨) [1]

(1. Anhui Meteorological Observatory, Hefei 230031 China; 2. Anhui Institute of Meteorological Sciences, Hefei 230031 China; 3. Anhui Province Key Laboratory of Atmospheric Science and Satellite Remote Sensing, Hefei 230031 China. 4. Institute of Atmospheric Physics, Chinese Academy of Sciences, Beijing 100029 China; 5. University of Chinese Academy of Sciences, Beijing 100049 China)

Abstract: The impacts of different moisture profiles on the structure and vertical motion of squall lines were investigated by conducting a set of numerical simulations. The base state was determined by an observational sounding, with high precipitable water representing moist environmental conditions in the East Asian monsoon region. To reveal the impact of moisture at different levels, the moisture content at the middle and low levels were changed in the numerical simulations. The numerical results showed that more convective cells developed and covered a larger area in the high moisture experiments, which was characteristic of the convection during the Meiyu season in China. In addition, high moisture content at low levels favored the development of updrafts and triggered convection of greater intensity. This was demonstrated by the thermodynamic parameters, including Convective Available Potential Energy (CAPE), Lifted Index (LI), Lift Condensation Level (LCL), and Level of Free Convection (LFC). Dry air at middle levels led to strong downdrafts in the environment and updrafts in clouds. This could be because dry air at middle levels favors the release of latent heat, thereby promoting updrafts in clouds and downdrafts in the environment. Therefore, high relative humidity (RH) at low levels and low RH at middle levels favors updrafts in the cloud cores. Additionally, moist air at low levels and dry air at middle levels promotes the development of convective cells and the intensification of cold pool. The squall line can be organized by the outflow boundary induced by cold pool. The balance of cold pool and environmental wind shear is favorable for the maintenance and strengthening of squall lines.

Key words: squall line; numerical simulation; precipitable water; downdraft; latent heat; cold pool

CLC number: P445 **Document code:** A

https://doi.org/10.46267/j.1006-8775.2020.029

1 INTRODUCTION

In China, mesoscale convective systems (MCSs) often induce heavy precipitation, thunderstorms, high winds, and hail in large areas (Chen et al. [1]; Yang et al. [2]; Li et al. [3]). However, it is difficult to predict MCSs accurately because their initiation and development mechanisms are yet to be understood fully (Zheng et al. [4]; He et al. [5]; Houze [6]). Among MCSs, squall lines have attracted much attention because of their organized nature and the severe weather they induce (Liang and Sun [7]; Meng and Zhang [8]; Meng et al. [9-10]; Zheng et al. [11]; Yang and Sun [12]). Although many studies have investigated various aspects of squall lines in certain specific regions of the world, few have investigated the environmental conditions that favor squall lines in China. However, the environments for development and evolution of squall lines are diverse in various climate regions.

Given the warm and moist air in the East Asian monsoon region (Tao [13]), the environmental characteristics of squall lines differ considerably from those in North America (Meng et al. [10]; Zheng [11]). Many studies have investigated the environmental moisture of squall lines in North America (Bluestein and Jain[14]; Klimowski [15]; Parker and Johnson [16]), demonstrating that the precipitable water (PWAT) is 20–35 mm, which is consistent with the dry-environment cases in central east China (Zheng et al. [11]). However, most squall lines are characterized by high PWAT (~60 mm) in southern China (Meng and Zhang [8]; Meng et al. [9]) and central east China (Meng et al. [10]; Zheng et al. [11]). A major difference between the dry and moist cases is the severe weather events that they bring. The MCS-induced severe weather differ significantly between dry and moist environments. High winds and hail events are observed mainly in dry environments, whereas short-term intense precipitation occur more frequently in moist environments (Zheng et al. [11]). In

Received 2019-12-16 **Revised** 2020-05-15 **Accepted** 2020-08-15

Funding: National Natural Science Foundation of China (41705029, 41675045); Strategic Priority Research Program of Chinese Academy of Sciences (XDA17010105); Key R&D Projects of Anhui Province (201904a07020099)

Biography: ZHENG Lin-lin, Ph. D., primarily undertaking research on mesoscale meteorology.

Corresponding author: SUN Jian-hua, e-mail: sjh@mail.iap.ac.cn

addition, the synoptic and surface circulations that trigger MCSs are different in dry and moist environmental conditions (Zheng and Sun [17]). It is therefore necessary to investigate the impacts of moisture on squall lines in the East Asian monsoon region (in the present study, we focus on east China) and the mechanisms behind those impacts.

Many studies have investigated the impacts of moisture on MCSs. Weisman and Klemp [18] (hereinafter WK82) demonstrated that the moisture at low levels has a considerable impact on the convective available potential energy (CAPE). Other observational and numerical results have shown that dry air has a significant impact on the strength of MCSs. Dry air conditions at middle levels lead to strong downdrafts, producing high surface winds and cold pools (Zipser [19]; Ogura and Liou [20]). Observational studies have verified the results and have suggested the associated mechanism (Lu et al. [21]), namely that lower relative humidity (RH) attenuates entrainment by increasing the buoyancy in the cloud cores and by strengthening the downdrafts near the cloud cores. However, some studies believed that dry air at middle levels accelerates the evaporation of precipitation parcels in convection, which is unfavorable for the development of cumulous convection (Brown and Zhang [22]; Redelsperger [23]; Ridout [24]; Takemi [25]). These studies focused mainly on the impacts of moisture on MCSs in either dry or tropical environments. However, the impacts of moisture on MCSs, especially squall lines, in eastern China remain to be investigated.

Some studies focused on how the moisture profile affects the evolution and organization of squall lines (Takemi [26-28], hereinafter T06 [26], T07a [27], and T14 [28], respectively). T06 [26] and T07a [27] suggested that moister conditions in the boundary layer are more favorable for squall line strength increase than moister conditions above the boundary layer do, as long as the overall available column moisture is similar. The moisture profiles used in Takemi [26], Takemi [27], and Takemi [28] were determined mostly based on analytical sounding (WK82 [18]), which represented typical conditions for convective storms over the continental plains of the United States. However, as is well known, the environmental conditions in China differ from those in the United States. Therefore, the effects of environmental moisture on the structure and intensity of squall lines, especially based on observations in China, need to be investigated. Squall line is a special subset of MCSs. How the MCSs line up is an issue being studied for a long time. Many previous studies have investigated the important roles of boundary convergence line on the initiation of convection, especially for squall lines (Carbon et al. [29]; Zhang et al. [30]). Boundary convergence lines include cold front, dry line, sea-land wind convergence zone, outflow boundary (gust front) and convergence zone caused by inhomogeneous spatial distribution of surface characteristics such as soil moisture (Wilson and Schreiber [31]; Wilson et al. [32]). Additionally, many studies investigated squall line related to tropospheric shear (Parker and Johnson [16]; LeMone et al. [33]; Johnson et al. [34]). The relationship between squall line and environmental shear is complex. Some squall lines are parallel to the shear, while others are perpendicular (Johnson et al. [34]).

In addition, many simulated studies have revealed that the role of vertical wind shear is one of the important ingredients in the squall line dynamics (Rotunno et al. [35]; Weisman et al. [36]; Fovell and Ogura [37]). Zheng and Sun [38] demonstrated that changing the vertical wind shear in the entire layer had the greatest impacts on the intensity and organizational mode of MCSs in eastern China. Therefore, the remaining question is how the squall lines sustain. There is an influential theory known as Rotunno-Klemp-Weisman (RKW) theory (Rotunno et al. [35]; Weisman [39]; Weisman and Rotunno [40]). The theory is that in the balance of horizontal vorticity induced by environmental shear and cold pool, the squall lines can sustain.

The impacts of the vertical distribution of moisture on MCSs will be discussed in the present paper. The purpose of the present study is to investigate the sensitivity of the initiation and vertical motion of squall lines to the vertical profile of moisture in eastern China. We conduct a set of idealized numerical experiments on squall lines under conditions with various vertical profiles of moisture using a non-hydrostatic model at a convection-resolving resolution. In section 2, we introduce the numerical model and the design of the moisture profiles in each experiment. The results of the experiments are discussed in section 3, and finally, the conclusions and discussions are given in section 4.

2 NUMERICAL MODEL AND EXPERIMENTAL DESIGN

The atmospheric model used in the present study was a version of the Weather Research Forecasting (WRF) model, namely the Advanced Research WRF (ARW) model (version 3.3), which was a non-hydrostatic compressible atmospheric model. The numerical experiments were configured for an observed sounding with idealized numerical experiments. The idealized experimental design used in the present study followed that of Weisman and Rotunno [40], T06 [26], T07a [27], Takemi [41] (hereinafter T07b [41]), Takemi [42] (hereinafter T10), and T14 [28]. The idealized experiments were configured with no Coriolis force, no surface fluxes, and no atmospheric radiation. The microphysics scheme was the Lin scheme, which was a sophisticated scheme that integrated ice, snow, and graupel processes. The grid spacing in the numerical experiments was 2 km in the horizontal direction and 41 levels in the vertical direction. The computational domain was 360 km (east-west, referred to as the *x*-axis) by 360 km (north-south; y-axis) by 18 km (vertical; z-axis). The boundary conditions were open at the east, west, south, and north boundaries. The lower boundary was free slip while the upper boundary was rigid, with a Rayleigh-type dumping layer imposed at the upper 5 km layer, in accordance with T14 [28].

The East Asian summer monsoon brings warm and moist air from the Indian and Western Pacific Ocean to east China (Tao [13]); short-term intense precipitation events tend to be associated with PWAT greater than 50 mm (defined as a moist environment), whereas PWAT less than 50 mm (defined as a dry environment) favors the generation of high winds and hail events (Zheng et al. [11]). Numerical experiments were conducted on a squall line that developed in dry environment and produced high winds and hail which occurred from June 3 to June 4, 2009 in the Henan, Anhui, and Jiangsu provinces of China (Sun et al. [43]). The results of that study showed that linear MCSs and high winds tended to occur when the mid-level air was dry and there was moist air at low levels.

To investigate the impacts of vertical distribution of moisture on the intensity, development, morphology, and vertical motion of MCSs in moist environments, a sounding in a moist environment was selected with which to perform idealized simulations. The base state was determined by using the observed sounding from Jinan station in Shandong province at 0000 UTC August 8, 2010 modified by the surface temperature from Lingxian County station observed at 0600 UTC, hereinafter referred to as the modified sounding (Fig. 1a). This modified-sounding technique was based on Johnson and Bresch [44], Pan et al. [45]. The modified sounding was characterized by high CAPE (4471 J kg^{-1}) and PWAT (68 mm) and high moisture at low levels (PWAT= 32 mm for heights of 1.5 km down to the surface). This sounding for all the experiments represented the major characteristics of the moist environmental conditions (Table 1 in Zheng et al. [11]). High hourly precipitation (102 mm) was observed near Lingxian County station during 2200–2300 UTC August 8, 2010 (figure not shown).The observed rainfall amount from 1200 UTC on 8 August to 0300 UTC on 9 August 2010 are shown in Fig. 2.

In accordance with the WK82 [18] sounding, the disturbance in the experiments was a warm bubble located at the center of the model region, 1.5 km above the surface, and with a horizontal diameter of 10 km and a vertical diameter of 1.5 km. In other words, the center of the bubble was located 1.5 km above the surface. The temperature perturbation of the bubble was calculated (when $\beta \leqslant 1$) by

$$\Delta T = T_0 \times \cos^2(\beta\pi/2), \quad (1)$$

where T_0=3K is the amplitude of the temperature perturbation and

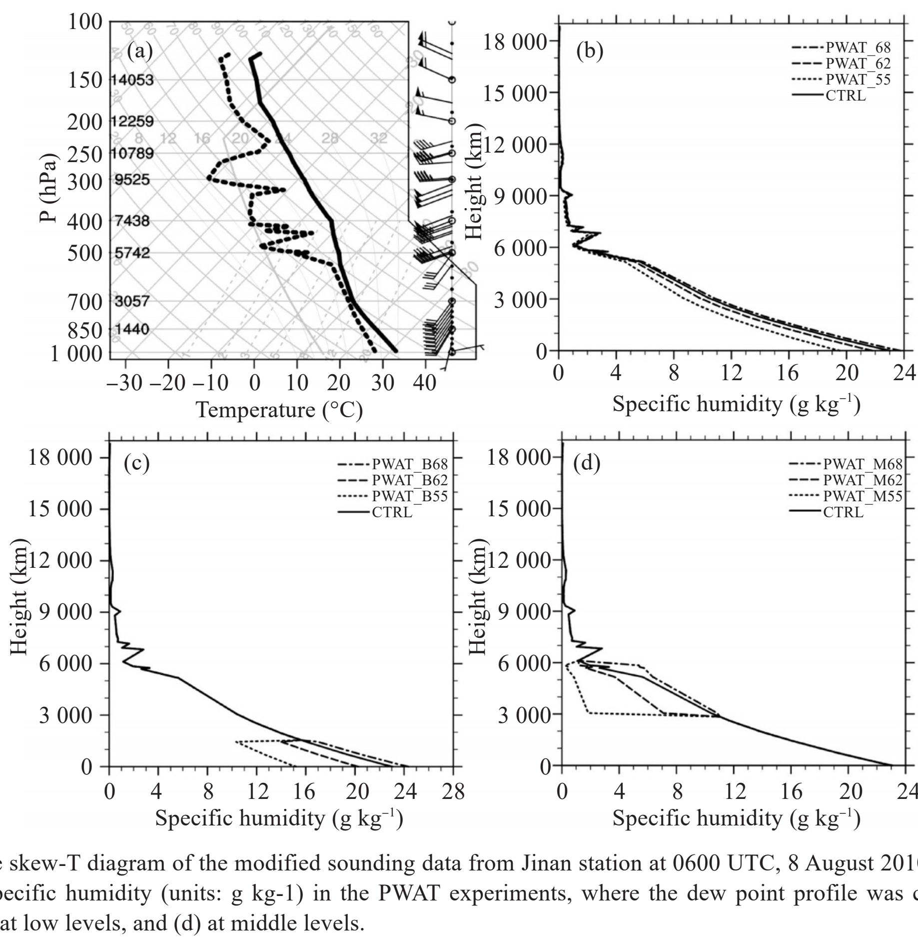

Figure 1. (a) The skew-T diagram of the modified sounding data from Jinan station at 0600 UTC, 8 August 2010; (b, c, d) The vertical profiles of specific humidity (units: g kg-1) in the PWAT experiments, where the dew point profile was changed over (b) the whole levels, (c) at low levels, and (d) at middle levels.

$$\beta = \sqrt{\left[\frac{(x - x_c)}{x_r}\right]^2 + \left[\frac{(y - y_c)}{y_r}\right]^2 + \left[\frac{(z - z_c)}{z_r}\right]^2}, \quad (2)$$

where x_r=y_r=10km and z_r=1.5km are the diameters of the bubble and (x_c, y_c, z_c) are the coordinates of its center.

Various moisture profiles were used in the experiments by changing the dew-point profile while the temperature profile remained unchanged. One reference experiment (CTRL) and nine experiments (PWAT) were conducted (Table 1). The dew-point profile was changed at all levels (Fig. 1b), at low levels (surface−1.5 km, Fig. 1c), or at middle levels (3−6 km, Fig. 1d). The specific method is to set a precipitable water value, change (increase or decrease) the dew point uniformly at the specified levels (eg. 3−6 km or surface−1.5 km) while keeping dew point at other levels not changing. Increase in the moisture content at all or low levels led to an increase in CAPE (Table 1), also shown in WK82 [18] and T07a [27]. By contrast, the thermodynamic parameters changed either a little or not at all when the moisture content was changed at middle levels (Table 1).

Table 1. The configurations (PWAT) and thermodynamic parameters of the CTRL and precipitation water (PWAT) experiments.

Experiments	PWAT (mm)			MUCAPE ($J\ kg^{-1}$)	MUCIN ($J\ kg^{-1}$)	LI (K)	LCL (m)	LFC (m)	PWAT
	Whole levels	Surface−1.5 km	3−6 km						
CTRL	66	32	13	4659	5	−9	767	1032	66
PWAT_68	68	33	16	5149	4	−9	703	939	68
PWAT_62	62	30	14	3863	8	−8	882	1214	62
PWAT_55	55	26	12	2448	15	−6	1110	1588	55
PWAT_B68	68	34	13	5541	3	−10	652	861	68
PWAT_B62	62	28	13	2855	13	−6	1035	1555	62
PWAT_B55	55	21	13	1148	78	−3	2243	2806	55
PWAT_M68	68	32	15	4652	5	−8	767	1032	68
PWAT_M62	62	32	9	4712	5	−9	767	1032	62
PWAT_M55	55	32	2	4774	5	−9	767	1032	55

Notes: MUCAPE, most unstable convective available energy; MUCIN, most unstable air parcel convective inhibition; LI, lifted index; LCL, lift condensation level; LFC, level of free convection.

3 RESULTS

3.1 *Structure and intensity of squall lines*

The characteristics of the structure and intensity of squall lines under different moisture profiles are investigated. The PWAT_55 and PWAT_B55 experiments failed to trigger convection during the simulation time period because of a weak unstable stratification at low levels, with a high level of free convection (LFC) and large most-unstable convective inhibition (MUCIN) of air parcels (Table 1). Consequently, the figures of those two experiments will not be shown in the follows. In the other experiments, convective cells that developed from the warm bubble generally became linearly organized (standard defined by Zheng et al. [11]) after 2 h of simulation, and linear systems oriented in the northwest-southeast direction developed after 4 h of simulation (figure not shown).

Composite radar reflectivity was used to demonstrate the structure of the squall lines. Fig. 3 shows the radar reflectivity at 5 h (the mature stage of convection) from the initial time of all experiments, except for PWAT_55 and PWAT_B55. More or / and larger convective cells developed in the high-moisture experiments (i. e., PWAT_68, PWAT_B68, and PWAT_M68) than in the low-moisture experiments (i.e., PWAT_62, PWAT_B62, PWAT_M62, and PWAT_M55). However, it is meaningful to compare similar PWAT experiments. Among the experiments with PWAT= 62 mm (i. e., PWAT_62, PWAT_M62, and PWAT_B62), the convection intensity was the strongest and the convectional area was the largest in PWAT_M62. This demonstrates that the intensity of convection is more sensitive to vertical distribution of moisture at low levels. Few studies have focused on the impacts of moisture profile on the intensity of convection, with the same PWAT over the whole levels. The present study demonstrates that the intensity of convection is sensitive to both the vertical distribution of moisture and the PWAT over the whole level.

As a measure of the intensity of squall lines, the vertical velocity at 3 km AGL at 5 h simulation time is shown in Fig. 4 for the PWAT experiments. The vertical velocity was relatively strong in the high moisture experiments (PWAT_68, PWAT_M68, and PWAT_B68) compared with the corresponding low moisture experiments (PWAT_M55, PWAT_M62, PWAT_62 and PWAT_B62). The vertical velocity was the strongest in PWAT_B68, and weakest in PWAT_B55 (not shown). The results indicate that the intensity of squall lines appeared more sensitive to moisture at low levels because of CAPE, lift condensation level (LCL) and

LFC (Table 1), which then affected the intensity of squall lines. This is consistent with WK82 [18].

The comparison among experiments with different PWAT was consistent with some studies (Brown and Zhang [22]; Redelsperger et al. [23]; Ridout [24]; Takemi et al. [25]), but inconsistent with other studies (Zipser [19]; Ogura and Liou [20]). However, it is meaningful to compare similar PWAT experiments. Few previous studies focused on comparing the impacts of the moisture profile on convection, but kept the PWAT over the whole level constant. Among the experiments with PWAT 62 mm, the vertical velocity in PWAT_M62 was stronger than that in PWAT_B62 (Fig. 4), indicating that the intensity of the squall lines was less sensitive to moisture at middle levels, and the moisture at low levels had the greatest impacts. Among the experiments with PWAT 68 mm, the vertical velocity was stronger in PWAT_B68 than in PWAT_M68, which indicated that stratification, with moist conditions at low levels and dry conditions at middle levels favored stronger convection intensities.

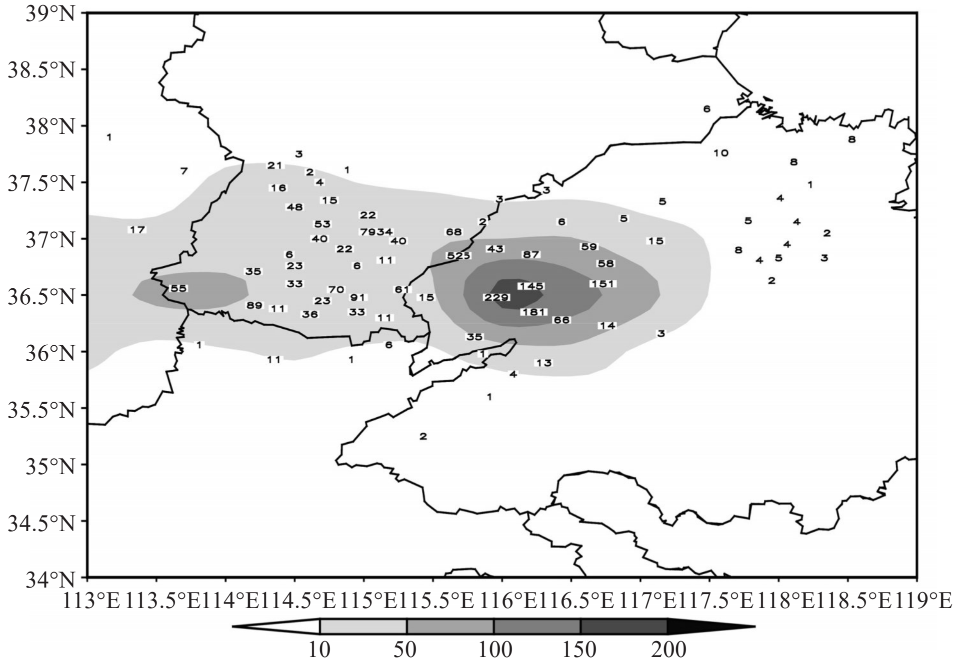

Figure 2. The observed rainfall (units: mm) from 1200 UTC on 8 August to 0300 UTC on 9 August, 2010.

Table 2. The 0–6 km wind shear, height and intensity of cold pool for PWAT_B68 and PWAT_M68 experiments.

	Height of cold pool (km)	Intensity of cold pool (m s^{-1})	0-6 km wind shear (m s^{-1})
PWAT_M68	1.1	13	16
PWAT_B68	1.3	16	16

3.2 *Updraft speed and precipitation intensity*

The updraft speed and precipitation intensity were calculated to demonstrate how the moisture profile affects squall lines, as done previously (Weisman et al. [36]; Weisman and Rotunno [40]; McCaul et al. [46]; T07a [27]; T10 [42]; T14 [28]). The mean and standard deviations of the model outputs for the areal maximum updraft speed and the maximum precipitation intensity were calculated statistically from 2 h to 12 h of the simulation period (Fig. 5a, b). The maximum updraft speed (Fig. 5a) was relatively large in the high-moisture experiments (i. e., PWAT_68, PWAT_M68, and PWAT_B68) and relatively small in the low-moisture experiments (i.e., PWAT_M55, PWAT_62, PWAT_M62, and PWAT_B62). The maximum updraft speed was most sensitive to moisture at low levels, as demonstrated by PWAT_B62 and PWAT_B68, which is consistent with the reflectivity intensity analyses in section 3.1. Because changes in the moisture content at low levels had the greatest impacts on the thermodynamical parameters, CAPE, LI, LCL, and LFC differed greatly between PWAT_B62 and PWAT_B68 (Table 1).

The vertical distribution of the areal maximum updraft speed is shown in Fig. 6a, demonstrating that updraft speed was generally the strongest in PWAT_B68 followed by PWAT_68 and CTRL, and weakest in PWAT_B62 (Fig. 6a). This distribution indicates that there were large differences in the updraft speed at 7–11 km above ground level (AGL) among different experiments, where the largest updraft speed was located

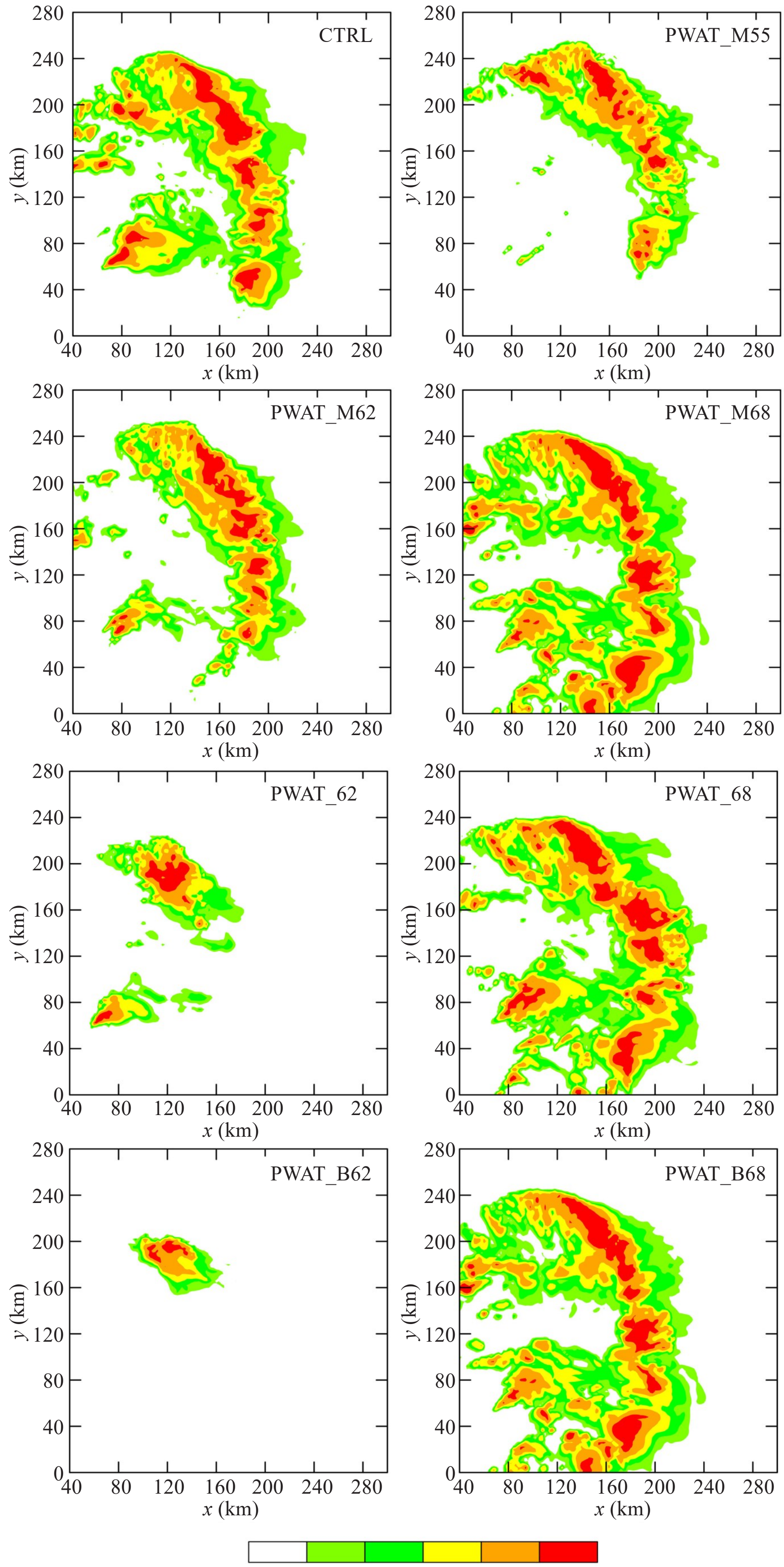

Figure 3. The composite radar reflectivity (units: dBZ) of the CTRL and precipitation water (PWAT) experiments at 5 h.

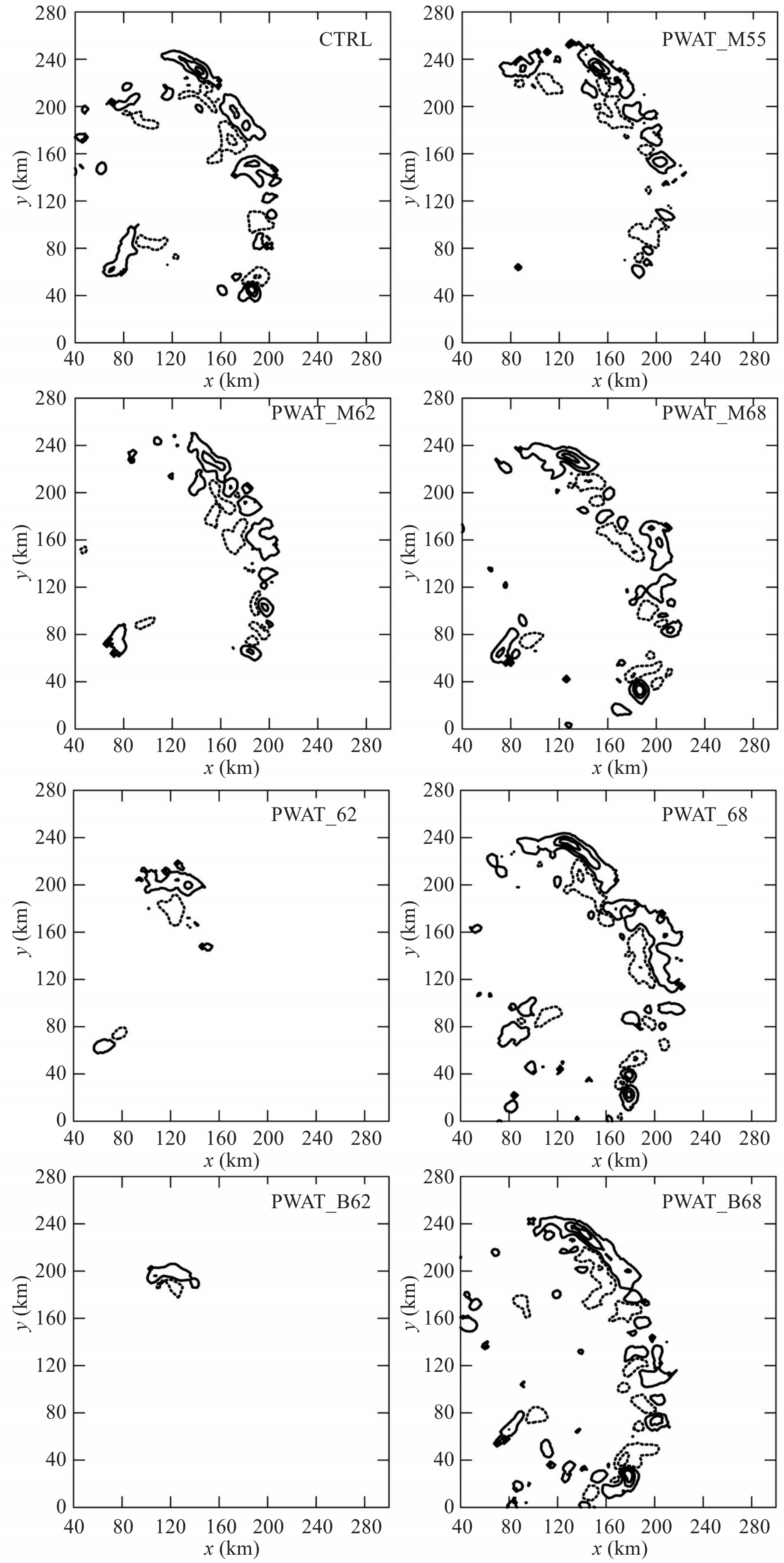

Figure 4. The updraft velocity (units: m s^{-1}; values of contours: −7, −4, −1, 1, 4 and 7 m s^{-1}) in the CTRL and precipitation water (PWAT) experiments after 5 h of simulation, at 3 km AGL.

and where Seeley and Romps [47] suggested that the buoyancy was the strongest. The proportional areal coverage of updraft was calculated as the number of grid cells with an updraft speed greater than or equal to 1 m s^{-1} divided by the total number of grid cells simulated. The areal coverage of updraft was the greatest in the high-moisture experiments (i. e., PWAT_68 and PWAT_B68) above 2 km AGL, and the areal coverage of updraft in PWAT_M68 was less than those in PWAT_68 and PWAT_B68 (Fig. 6b). This indicates that high moisture at low levels favors the initiation of convection. The updraft speed was stronger in PWAT_B68 and PWAT_M62 than that in PWAT_M68 and PWAT_B62, respectively (Fig. 6a), thereby indicating that moisture concentrated at low levels (Fig. 1c, d) favors the development of convective updraft.

Corresponding to the updraft speed, the maximum precipitation intensity (Fig. 5b) was relatively large in the high-moisture experiments (i. e., PWAT_68, PWAT_M68, and PWAT_B68) and relatively small in the low-moisture experiments (i. e., PWAT_M55, PWAT_M62, PWAT_62, and PWAT_B62). Under similar CAPE and high-PWAT conditions (i. e., PWAT_68, PWAT_B68, and PWAT_M68; Table 1), the precipitation intensity was roughly the same. The largest differences in areal maximum precipitation were those between PWAT_B68 and PWAT_B62 (Fig. 5b). These results are consistent with T10 [42], which demonstrated that the maximum precipitation intensity was regulated by moisture in the tropospheric lower layer. In general, the stability of the atmosphere was affected most by moisture at low levels. The moisture content at low levels had a significant effect on the updraft speed, which in turn had large impacts on the initiation of squall lines and on their intensity and precipitation.

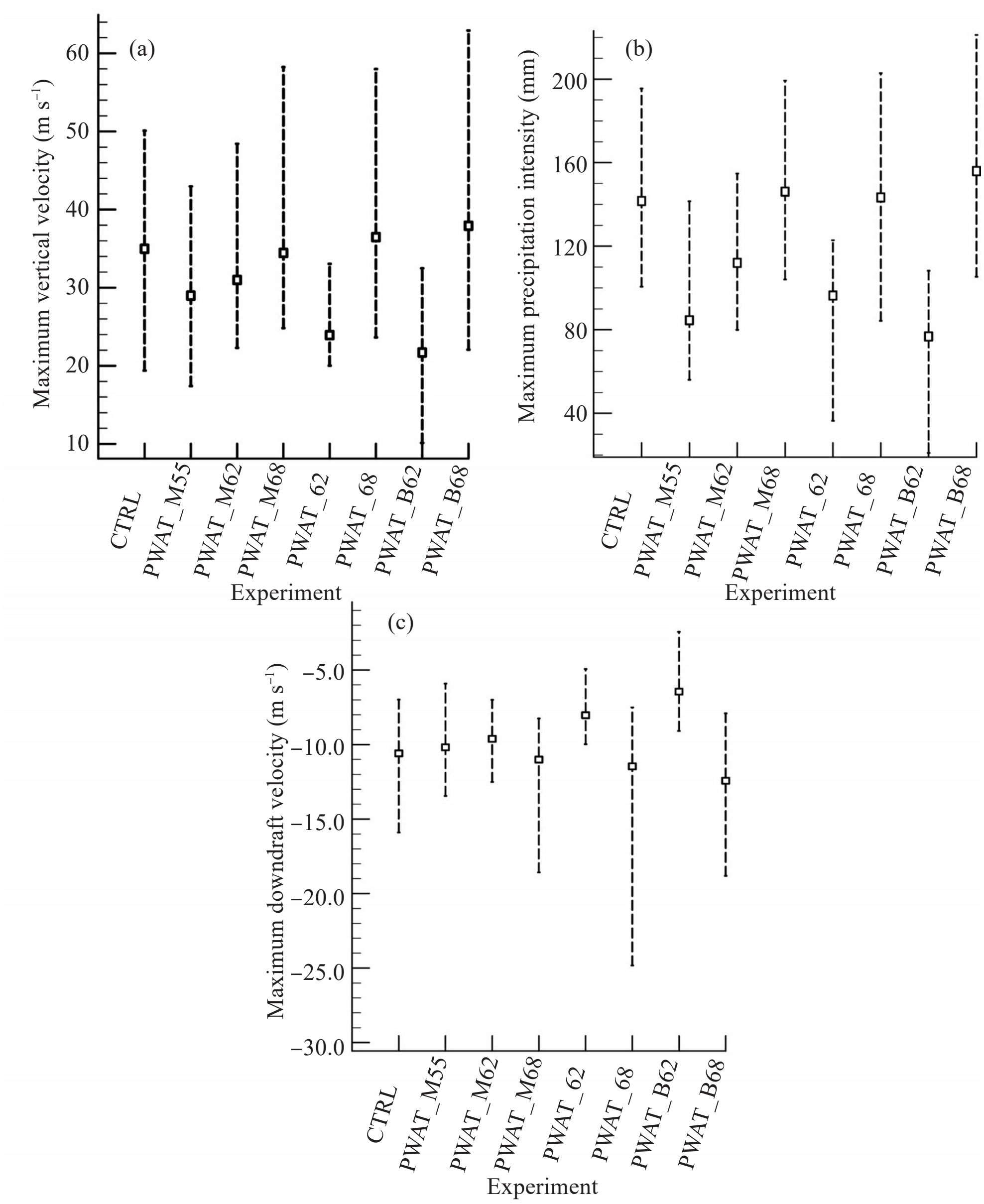

Figure 5. The mean (boxes) and standard deviation (bars) of (a) the maximum updraft speed, (b) the maximum precipitation intensity, and (c) the maximum downdraft speed, across the computational domain from 2 to 12 h for each numerical experiment.

3.3 *Downdraft speed*

The downdraft speed was investigated to show the impacts of moisture profiles on squall lines, because there are different views on how dry air at middle levels affects the convection intensity, as mentioned in section 1. Fig. 5c shows the mean and standard deviation of the areal maximum downdraft speed, averaged over the simulated domain from 2 to 12 h of the simulation period. Generally, the downdraft speed was strong in the high-moisture experiments (i. e., PWAT_68, PWAT_M68, and PWAT_B68) and weak in the low-moisture experiments (i. e., PWAT_62, PWAT_M62, PWAT_B62, and PWAT_M55) (Fig. 5c). The downdrafts were the strongest in PWAT_M55 among the low-moisture experiments and in PWAT_B68 among the high-moisture experiments. This indicates that dry air at middle levels and moist air at low levels can lead to stronger downdrafts. In particular, the maximum downdraft speed was larger in PWAT_M55 than in PWAT_M62, which indicates that the strength of downdraft velocity was not only affected by PWAT, especially with drier conditions at middle levels. Fig. 5c shows the maximum downdraft, which can be located at different levels, thereby making it necessary to investigate the downdraft profiles.

The vertical profiles of maximum downdraft speeds and their areal coverage are shown in Fig. 6c, d, respectively. The maximum downdraft speeds located at 3–4 km AGL, resulting in the maximum areal coverage at 2–3 km AGL. The downdraft speed and its areal coverage dropped sharply below 3 and 2 km AGL, respectively. The downdraft speed is not only affected by PWAT, but also by the profile of specific humidity. For a given PWAT, the downdraft speed was the largest in PWAT_B68 and smallest in PWAT_M68 in the high-moisture experiments but the largest in PWAT_M55 and the smallest in PWAT_B62 in the low-moisture experiments. The profile of specific humidity showed moist middle levels with dry low levels in PWAT_M68 and PWAT_B62 and dry middle levels with moist low levels in PWAT_B68 and PWAT_M62 (Fig. 1c, d). Therefore, the results indicate that an environment with dry middle levels and moist low levels favors higher downdraft, especially so for the dry middle levels (e.g., PWAT_M55). Moreover, the maximum downdraft speed in PWAT_M55 was located at lower levels (2–3 km AGL) than that in PWAT_B68 (3–4 km AGL), and below the maximum height the downdraft speed decreased more slowly in PWAT_M55. This indicates that a dry environment favors downdrafts being sustained at middle-to-low levels, which may be a reason for the associated high surface wind.

4 THEORETICAL DISCUSSION

4.1 *Impact of sensible heat and latent heat on buoyancy*

We have shown that moisture located at low levels favors the development of convective updrafts, while dry air at middle levels favors downdrafts being sustained at middle-to-low levels. Lu et al. [21] suggested that positive correlations existed between cloud buoyancy and W_c (W in the cloud cores, hereinafter referred to as updraft). In addition, a larger downdraft (more negative W_e) corresponds to a larger updraft, which may be related to the coherent structures or internal circulations between updrafts and downdrafts (Park et al. [48]; Sherwood et al. [49]). Buoyancy is a physical parameter that reflects the updraft intensity in cumulus clouds (Lu et al. [21, 50]), namely

$$B = \frac{T_{vc} - T_{ve}}{T_{ve}} g \tag{3}$$

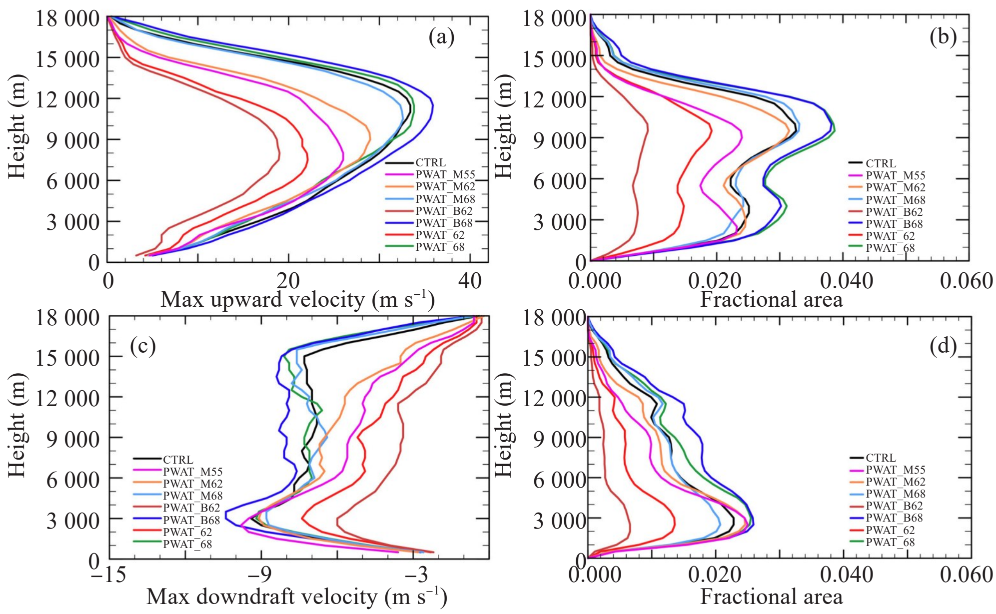

Figure 6. The temporally averaged vertical profiles of (a) the maximum updraft speed, and (b) the fractional area of updraft, (c) the maximum downdraft speed and (d) the fractional area of downdraft, from 2 to 12 h for each numerical experiment.

where g is the acceleration due to gravity and T_v is the virtual temperature (Wallace and Hobbs[53]), and $T_v = T\left(1 + 0.608q_v\right)$. Here, T_{vc} is the maximum temperature in cloud and T_{ve} is the average temperature of a 20 km× 20 km area located 40 km away from the edge of the cloud core where there is no contamination due to convection.

As shown in Fig. 7a, the buoyancy below 3 km AGL was the largest in PWAT_B68, while the buoyancy at 3–6 km AGL was the largest in PWAT_M55. Being consistent with Lu et al. [50], negative correlation between buoyancy and RH in the middle levels of troposphere was verified in PWAT_M55, PWAT_M62, and PWAT_M68. RH affects cloud buoyancy through its impacts on the evaporation rate of cloud droplets, and then the lower temperature in environments affects the cloud buoyancy (Lu et al. [50]). By contrast, buoyancy and RH at tropospheric low levels have positively correlations, and this may because of that buoyancy energy, such as CAPE (Table 1) increases with low-level moisture, which is also demonstrated by T06[26]. The vertical profiles of buoyancy demonstrated that high RH at low levels and low RH at middle levels favor updraft in the cloud cores. Consequently, low RH at middle levels favors high downdrafts in environments, which is suggested by the mechanism of coherent structures or internal circulations between updrafts and downdrafts (Park et al. [48]; Sherwood et al. [49]).

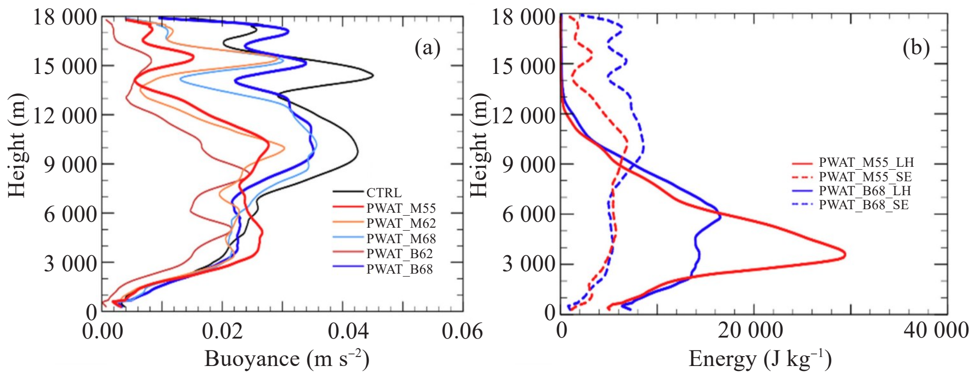

Figure 7. Vertical profiles of (a) buoyancy, and parcel-environment differences of (b) latent enthalpy (blue lines) and sensible heat (red lines) for 5h integration of each numerical experiment.

The mechanism of RH at middle levels negatively correlated with buoyancy can be explained by the parcel-environment difference in moist static energy (MSE) ($\Delta h = C_p\Delta T + L\Delta q_v$, Seeley and Romps[47]). This is because the RH influences the updraft in clouds, and updraft is driven by two processes, namely parcel-environment differences in sensible heat (SH) and latent enthalpy (LH). Here, Δh, ΔT, and Δq_v are the differences in MSE, temperature, and specific humidity, respectively, between clouds and environments. $C_p\Delta T$ is a parcel-environment difference term known as the SH, and $L\Delta q_v$ is the LH. As shown in Fig. 7b, the parcel-environment differences of LH at 3–6 km AGL was larger in PWAT_M55 than in PWAT_B68. The result indicated that dry environmental air at middle levels can generate faster and stronger evaporation cooling in environment, which led to larger parcel-environment differences of temperature. These results are consistent with those of Lu et al. [50] that more dry air promotes downdrafts in environments as well as updrafts in clouds induced by the coherent structure between updraft and downdraft (Park et al. [48]; Sherwood et al. [49]). However, the parcel-environment differences of latent heat at low levels in PWAT_B68 was slightly larger than that in PWAT_M55 (Fig. 7b). This indicates that the impacts on buoyancy at low levels are more complex because of complex near-surface physical processes. For example, the downdraft and evaporation of a convection line produce cold pool near the surface. However, the temperature and moisture in environments are represented herein by those in the area uncontaminated by convection, so the role of cold pools was not considered. Moreover, cold pools can have opposite effects on convection in different stages (e.g., active and suppressed). For example, Feng et al. [51] showed that the characteristics of cold pools can trigger new convection. Convectively generated cold pools can suppress convection by cooling and / or drying the surface and boundary layers during suppressed convections stages (Chen et al. [52]).The roles of cold pools are complex and should be studied further, but the present paper focuses more on the impacts of environmental moisture, i.e., that uncontaminated by convection.

4.2 *The formation and development of squall line*

For the same PWAT experiments, environmental humidity profile has impact on the formation of squall line. The squall line was formed in PWAT_B62 experiment (Fig. 8a3), but was not formed in PWAT_M62 experiment (Fig. 8b3). As for PWAT_B62 experiment, high humidity and low pseudo phase temperature located at the lower levels associated with higher MUCAPE (Table 1) which leads to stronger convection and formation of cold pool. At the junction of cold pool and ambient air, a new cell B is triggered

(Fig. 8a1). The superimposition of B and A's cold pool increased the strength and range of the original cell A, and then triggered new cells C and D (Fig. 8a2, a3). The continuously triggered cells arranged in a line along outflow boundary of cold pool. The intensity of initial convection and cold pool are strong enough (Fig. 8), leading to convergence line between the cold pool and the environmental air; at the convergence line, new cells are constantly triggered and organized into squall lines, which is also noted by Wilson et al. [32].

The intensity of squall line is also affected by vertical distribution of humidity (T06 [26], T07a [27], and T14 [28]). For the same PWAT experiment, the intensity of squall line is stronger in PWAT_B68 experiment than that in PWAT_M68 experiment (Fig. 3, 4, 5). On the one hand, the high humidity located at the lower levels is conducive to the enhancement of upward velocity (Fig. 9d) and positive buoyancy (Fig. 7a), which leads to stronger convective cells. On the other hand, the middle level dry air favored the strengthening of cold pool,

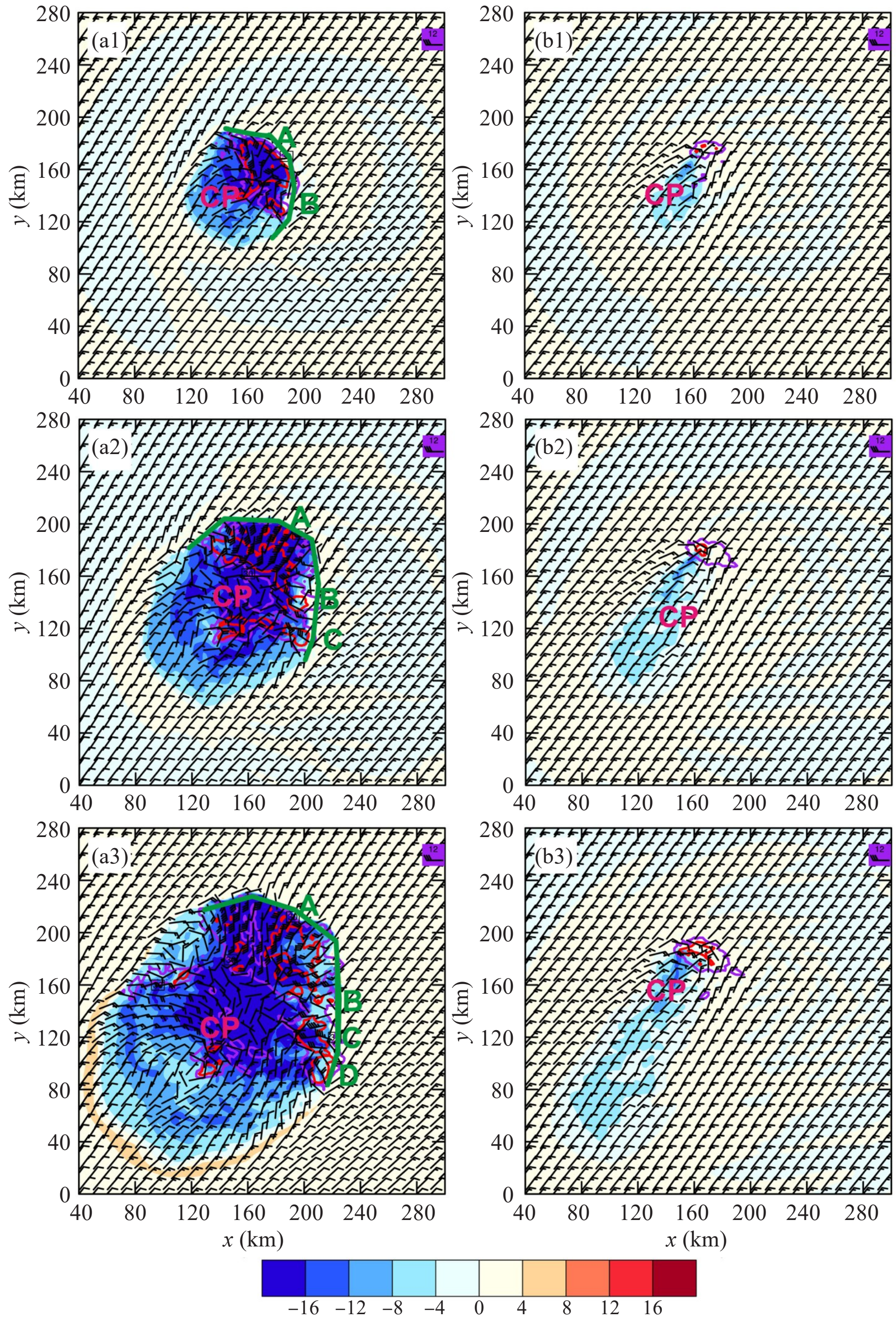

Figure 8. The perturbation of equivalent potential temperature (shaded, units: K), horizontal wind (barb, full barb represents 4 m s^{-1}) at 500m above ground level and the composite reflectivity (contour, units: dBZ) for 2h (a1, b1), 3h (a2, b2) and 4h (a3, b3) integration of PWAT_M62 (a1, a2, a3) and PWAT_B62 (b1, b2, b3) experiments. The green solid lines in a1, a2 and a3 represent convergence line in front of cold pool.

which is verified by result that PWAT_B68 expriment has a stronger cold pool (blue area in Fig. 9a, b, purple dotted part in Fig. 9c, d). The stronger cold pool is favorable for triggering new convection. According to RKW theory (Rotunno et al. [35]; Weisman [39]; Weisman and Rotunno [40]), when the horizontal vorticity induced by the intensity of cold pool and vertical wind shear become to a balance, it is most beneficial to maintain the squall line. The 0–6 km wind shear in PWAT_M68 and PWAT_B68 experiment is 16 m s^{-1}, and the strength of cold pool in PWAT_B68 experiment is equivalent to that of wind shear, while the strength of cold pool in PWAT_M68 experiment is smaller than that of wind shear (Table 2).

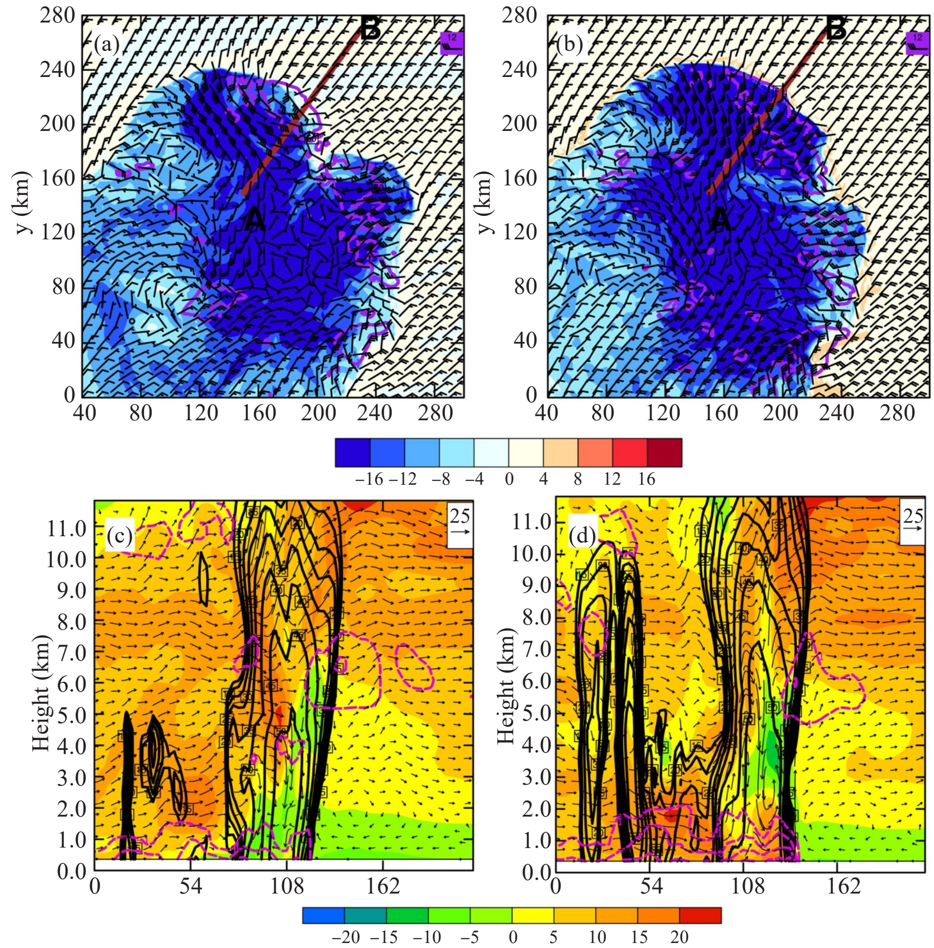

Figure 9. The same as Fig. 8, but for 5h integration of (a) PWAT_M68 and (b) PWAT_M68 experiment. Composite reflectivity (black contour, units: dBZ), negative perturbation of pseudo-equivalent potential temperature (purple dashed line, units: K), horizontal wind speed (shaded area, units: m s^{-1}) and wind vector (arrow, units: m s^{-1}, vertical wind speed amplified 10 times) at AB cross section in (a) and (b) for 5h integration of (c) PWAT_M68 and (d) PWAT_M68 experiment.

5 SUMMARY AND DISCUSSION

By conducting idealized numerical simulations based on an observational sounding, the present study investigated the sensitivities of the initiation and intensity of squall lines to different moisture profiles in east China. Based on the studies of T06 [26], T07a [27], and T14 [28], we focused specifically on moisture profiles that represented wet environmental conditions in east China. The results showed that the initiation and intensity of squall lines are very sensitive to the vertical distribution of moisture.

The moisture at different levels has complicated impacts on the stabilities of the atmosphere and squall lines. In high-moisture experiments with the low-moisture ones, more convective cells developed and covered a larger area in the high-moisture experiments, which is characteristic of the convection during the Meiyu season in China. Nevertheless, the initiation of convection was more sensitive to moisture at low levels. This was demonstrated by the thermodynamic parameters (CAPE, LI, LCL, and LFC).

As for updraft in clouds, it was relatively strong in the high moisture experiments compared with that in corresponding low moisture experiments. In addition, with the same PWAT, the intensity of squall lines was more sensitive to moisture at low levels than that at middle levels. Corresponding to the updraft, the precipitation intensity was strong in the high moisture experiments and weak in the low moisture experiments. In environments with more moist air at low levels, stratification becomes more unstable (Table 1), and buoyancy increases with the increase of low level humidity.

In general, the maximum downdraft as well as updraft speed occurred in environments with high PWAT, which may be related to the coherent structures or internal circulations between updrafts and downdrafts. However, the downdraft speed is affected by more than just PWAT: dry middle levels can also lead to downdrafts being sustained at middle-to-low levels, even with low PWAT. Dry middle levels favor stronger downdrafts because dry air at middle levels favors the release of latent heat, which promotes updrafts in clouds and downdrafts in environments.

Moist air at low levels is favorable for the formation of squall line, which is mainly induced by the formation or enhancement of boundary layer convergence line. The reason may be that low-level moisture can strengthen both convective updraft and cold pool and dry middle-level moisture enhances cold pool. The outflow boundary of cold pool is a type of boundary layer convergence line which can organize squall line. The balance of cold pool and environmental wind shear favored the maintenance of squall line, which is consistent with RKW theory. Thus, moist air at low levels and dry air at middle levels are conductive to the maintenance and strengthening of squall line.

The present study focused on moist environmental conditions in China, and the numerical simulations also indicated that the intensity of squall lines is affected significantly by moisture at low levels and that dry air at middle levels favors the formation of squall lines. The mechanisms behind these trends should be investigated further. However, squall lines probably develop during dry environmental conditions in China. Therefore, the impacts of thermodynamics on squall lines under dry environmental conditions should also be investigated in east China and compared with results from the United States.

REFERENCES

[1] CHEN Jiong, ZHENG Yong-guang, ZHANG Xiao-ling, et al. Distribution and diurnal variation of warm-season short-duration heavy rainfall in relation to the MCSs in China [J]. J Meteor Res, 2013, 27(6): 868-888, https://doi. org / 10.1007/s13351-013-0605-x.

[2] YANG X L, SUN J H, ZHENG Y G. A 5-yr climatology of severe convective wind events over China [J]. Wea Forecasting, 2017, 32(4): 1289-1299, https://doi. org / 10.1175/WAF-D-16-0101.1.

[3] LI X, ZHANG Q, ZOU T, et al. Climatology of hail frequency and size in China, 1980-2015 [J]. J Appl Meteor Climatol, 2018, 57(4): 875-887, https://doi. org / 10.1175 / JAMC-D-17-0208.1.

[4] ZHENG Yong-guang, ZHANG Xiao-ling, ZHOU Qin-liang, et al. Review on severe convective weather short-term forecasting and nowcasting [J]. Meteor Mon, 2010, 36 (7): 33-42 (in Chinese).

[5] HE Li-fu, ZHOU Qing-liang, CHEN Yun, et al. Introduction and examination of potential forecast for strong convective weather at national level [J]. Meteor Mon, 2011, 37(7): 777-784 (in Chinese).

[6] HOUZE R A. 100 years of research on mesoscale convective systems [J]. Meteor Monogr, 2018, 59: 171-1754, https://doi.org/10.1175/AMSMONOGRAPHS-D-18-0001.1.

[7] LIANG Jian-yu, SUN Jian-hua. The formation mechanism of damaging surface wind during the squall line in June 2009 [J]. Chin J Atmos Sci, 2012, 36(2): 316-336 (in Chinese).

[8] MENG Z, ZHANG Y. On the squall lines preceding landfalling tropical cyclones in China [J]. Mon Wea Rev, 2012, 140(2): 445-470, https://doi. org / 10.1175 / MWR-D-10-05080.1.

[9] MENG Z, ZHANG F, MARKOWSKI P, et al. A modeling study on the development of a bowing structure and associated rear inflow within a squall line over south China [J]. J Atmos Sci, 2012, 69(4): 1182-1207, https://doi. org / 10.1175/JAS-D-11-0121.1.

[10] MENG Z, YAO D, ZHANG Y. General features of squall lines in east China [J]. Mon Wea Rev, 2013, 141(5): 1629-1647, https://doi.org/10.1175/mwr-d-12-00208.1.

[11] ZHENG L, SUN J, ZHANG X, et al. Organizational modes of mesoscale convective systems over central east China [J]. Wea Forecasting, 2013, 28(5): 1081-1098, https://doi.org/10.1175/WAF-D-12-00088.1.

[12] YANG X, SUN J. Organizational modes of severe wind-producing convective systems over North China [J]. Adv Atmos Sci, 2018, 35(5): 540-549, https://doi.org/10.1007/ s00376-017-7114-2.

[13] TAO Shi-yan. Heavy Rainfalls in China [M]. Beijing: Science Press, 1980 (in Chinese).

[14] BLUESTEIN H B, JAIN M H. Formation of mesoscale lines of precipitation: severe squall lines in Oklahoma during the spring [J]. J Atmos Sci, 1985, 42(16): 1711-1732, https://doi.org/10.1175/1520-0493(1987)115<2719: FOMLOP>2.0.CO;2.

[15] KLIMOWSKI B A, BUNKERS M J, HJELMFELT M R, et al. Severe convective windstorms over the Northern High Plains of the United States [J]. Wea Forecasting, 2003, 18(3): 502-519, https://doi. org / 10.1175 / 1520-0434 (2003)18<502:SCWOTN>2.0.CO;2.

[16] PARKER M D, JOHNSON R H. Organizational modes of midlatitude mesoscale convective systems [J]. Mon Wea Rev, 2000, 128(10): 3413-3436, https://doi. org / 10.1175 / 1520-0493(2001)129<3413:OMOMMC>2.0.CO;2.

[17] ZHENG Lin-lin, SUN Jian-hua. Characteristics of synoptic and surface circulation of mesoscale convective systems in dry and moist environmental conditions [J]. Chin J Atmos Sci, 2013, 37(4): 891-904 (in Chinese), https://doi.org/10.3878/j.issn.1006-9895.2012.12090.

[18] WEISMAN M L, KLEMP J B. The dependence of numerically simulated convective storms on vertical wind shear and buoyancy [J]. Mon Wea Rev, 1982, 110(6): 504-520, https://doi. org / 10.1175 / 1520-0493(1982)110<0504: TDONSC>2.0.CO;2.

[19] ZIPSER E J. Mesoscale and convective-scale downdrafts

as distinct components of squall-line circulation [J]. Mon Wea Rev, 1977, 105(12): 1568-1589, https://doi. org / 10.1175 / 1520-0493(1977)105<1568: MACDAD>2.0. CO; 2.

[20] OGURA Y, LIOU M T. The structure of a midlatitude squall line [J]. J Atmos Sci, 1980, 37(3): 553-567, https:// doi. org / 10.1175 / 1520-0469(1980)037<0553: TSOAMS> 2.0.CO;2.

[21] LU C, SUN C, LIU Y, et al. Observational relationship between entrainment rate and environmental relative humidity and implications for convection parameterization [J]. Geophys Res Lett, 2018, 45(24): 13495-13504, https://doi.org/10.1029/2018GL080264.

[22] BROWN R G, ZHANG C. Variability of midtropospheric moisture and its effect on cloud-top height distribution during TOGA COARE [J]. J Atmos Sci, 1997, 54(23): 2760-2774, https://doi.org/10.1175/1520-0469(1997)054< 2760:VOMMAI>2.0.CO;2.

[23] REDELSPERGER J L, PARSONS D B, GUICHARD F. Recovery processes and factors limiting cloud-top height following the arrival of a dry intrusion observed during TOGA COARE [J]. J Atmos Sci, 2002, 59(16): 2438-2457, https://doi.org/10.1175/1520-0469(2002)059<2438: RPAFLC>2.0.CO;2.

[24] RIDOUT J A. Sensitivity of tropical Pacific convection to dry layers at mid-to upper levels: Simulation and parameterization tests [J]. J Atmos Sci, 2002, 59(23): 3362-3381, https://doi.org/10.1175/1520-0469(2002)059< 3362:SOTPCT>2.0.CO;2.

[25] TAKEMI T, HIRAYAMA O, LIU C. Factors responsible for the vertical development of tropical oceanic cumulus convection [J]. Geo Res Lett, 2004, 31: L11109, https:// doi.org/10.1029/2004GL020225.

[26] TAKEMI T. Impacts of moisture profile on the evolution and organization of midlatitude squall lines under various shear conditions [J]. Atmos Res, 2006, 82(1-2): 37-54, https://doi.org/10.1016/j.atmosres.2005.01.007.

[27] TAKEMI T. A sensitivity of squall line intensity to environmental static stability under various shear and moisture conditions [J]. Atmos Res, 2007a, 84(4): 374-389, https://doi.org/10.1016/j.atmosres.2006.10.001.

[28] TAKEMI T. Convection and precipitation under various stability and shear conditions: Squall lines in tropical versus midlatitude environment [J]. Atmos Res, 2014, 142 (3): 111-123, https://doi. org / 10.1016 / j. atmosres.2013.07.010.

[29] CARBON R, BRANT FOOTE G, MONCRIEFF M, et al. Convective Dynamics: Panel Report [M]. Radar in Meteorology. Amer Meteor Soc. 1990, 391-400.

[30] ZHANG Qun, ZHANG Wei-hung, JIANG Yong-qian. Numerical trial of PBL convergence line developing to squall line [J]. Scientia Meteor Sinica, 2001, 21(3): 308-315 (in Chinese).

[31] WILSON J W, SCHREIBER W E. Initiation of convective storms by radar-observed boundary layer convergence lines [J]. Mon Wea Rev, 1986, 114(12): 2516-2536, https: //doi. org / 10.1175 / 1520-0493(1986)114<2516: IOCSAR> 2.0.CO;2.

[32] WILSON J W, ROBERTS R, MUELLER C. Forecast demonstration project: convective storm now casting [J]. Wea Forecasting, 2004, 19: 131-150.

[33] LEMONE M A, ZIPSER E J, TRIER S B. The role of environmental shear and thermodynamic conditions in determining the structure and evolution of mesoscale convective systems during TOGA COARE [J]. J Atmos Sci, 1998, 55(23): 3493-3518, https://doi. org / 10.1175 / 1520-0469(1998)055<3493:TROESA>2.0.CO;2.

[34] JOHNSON R H, AVES S L, CIESIELSKI P E, et al. Organization of oceanic convection during the onset of the 1998 East Asian summer monsoon [J]. Mon Wea Rev, 2005, 133(1): 131-148, https://doi. org / 10.1175 / MWR-2843.1

[35] ROTUNNO R, KLEMP J B, WEISMAN M L. A theory for strong, long-lived squall lines [J]. J Atmos Sci, 1988, 45(3): 463-485, https://doi.org/10.1175/1520-0469(1988) 045<0463:ATFSLL>2.0.CO;2.

[36] WEISMAN M L, KLEMP J B, ROTUNNO R. Structure and evolution of numerically simulated squall lines [J]. J Atmos Sci, 1988, 58(14): 1630-1649, https://doi. org / 10.1175/1520-0469(1988)045<1990:SAEONS>2.0.CO;2.

[37] FOVELL R G, OGURA Y. Effect of vertical wind shear on numerically simulated multicell storm structure [J]. J Atmos Sci, 1989, 46(20): 3144-3176, https://doi. org / 10.1175 / 1520-0469(1989)046<3144: EOVWSO>2.0. CO; 2.

[38] ZHENG Lin-lin, SUN Jian-hua. The impact of vertical wind shear on the intensity and organizational mode of mesoscale convective systems using numerical experiments [J]. Chin J Atmos Sci, 2016, 40 (2): 324-340 (in Chinese), https://doi. org / 10.3878 / j. issn. 1006-9895.1505.14311.

[39] WEISMAN M L. The role of convectively generated rear-inflow jets in the evolution of long-lived meso convective systems [J]. J Atmos Sci, 1992, 49(19): 1826-1847, https: //doi.org/10.1175/1520-0469(1992)049<1826:TROCGR> 2.0.CO;2.

[40] WEISMAN M L, ROTUNNO R. A theory for strong long-lived squall lines" revisited [J]. J Atmos Sci, 2004, 61(4): 361-382, https://doi. org / 10.1175 / 1520-0469(2004)061< 0361:ATFSLS>2.0.CO;2.

[41] TAKEMI T. Environmental stability control of the intensity of squall lines under low-level shear conditions [J]. J Geophys Res, 2007b, 112: D24110.

[42] TAKEMI T. Dependence of the precipitation intensity in mesoscale convective systems to temperature lapse rate [J]. Atmos Res, 2010, 96: 273-285.

[43] SUN Jian-hua, ZHENG Lin-lin, ZHAO Si-xiong. Impact of moisture on the organizational mode and intensity of squall lines determined through numerical experiments [J]. Chin J Atmos Sci, 2014, 38(4): 742-755 (in Chinese), https://doi.org/10.3878/j.issn.1006-9895.2013.13187.

[44] JOHNSON R H, BRESCH J F. Diagnosed characteristics of precipitation systems over Taiwan during the May-June 1987 TAMEX [J]. Mon Wea Rev, 1991, 119(11): 2540-2557.

[45] PAN Yu-jie, ZHAO Kun, PAN Yi-nong. Single-Doppler radar observation of a heavy precipitation supercell on a severe squall line [J]. Acta Meteor Sinica, 2008, 66(4): 621-636 (in Chinese).

[46] MCCAUL Jr, COHEN E W, KIRKPATRICK C. The sensitivity of simulated storm structure, intensity, and precipitation efficiency to environmental temperature [J]. Mon Wea Rev, 2005, 133: 3015-3037.

[47] SEELEY J T, ROMPS D M. Tropical cloud buoyancy is

the same in a world with or without ice [J]. Geophys Res Lett, 2016, 43: 3572-3579, https://doi. org / 10.1002 / 2016GL068583.
[48] PARK S B, GENTINE P, SCHNEIDER K. et al. Coherent structures in the boundary and cloud layers: Role of updrafts, subsiding shells, and environmental subsidence [J]. J Atmos Sci, 2016, 73(4): 1789-1814, https://doi.org/10.1175/jas-d-15-0240.1.
[49] SHERWOOD S C, HERNANDEZ-DECKERS D, COLIN M, et al. Slippery thermals and the cumulus entrainment paradox [J]. J Atmos Sci, 2013, 70(8): 2426-2442. https://doi.org/10.1175/JAS-D-12-0220.1.
[50] LU C, LIU Y, ZHANG G J, et al. Improving parameterization of entrainment rate for shallow convection with aircraft measurements and large eddy simulation [J]. J Atmos Sci, 2016, 73(2): 761-773, https://doi.org/10.1175/JAS-D-15-0050.1.
[51] FENG Z, HAGOS S, ROWE A K, et al. Mechanisms of convective cloud organization by cold pools over tropical warm ocean during the AMIE/DYNAMO field campaign [J]. J Adv Mod Earth Sys, 2015, 7(2): 357-381.
[52] CHEN S, KERNS B W, GUY N, et al. Aircraft observations of dry air, the ITCZ, convective cloud systems, and cold pools in MJO during DYNAMO [J]. Bull Amer Meteor Soc, 2016, 97(3): 405-423.
[53] WALLACE J, HOBBS P. Atmospheric Science: An Introductory Survey [M]. San Diego, CA: Academic Press, 2006.

Citation: ZHENG Lin-lin, SUN Jian-hua, ZHANG Jiao, et al. Squall line and its vertical motion under different moisture profiles in eastern China [J]. J Trop Meteor, 2020, 26(3): 321-335, https://doi.org/10.46267/j.1006-8775.2020.029.